

Flow of Micropolar Fluids over a Stretchable Disk

¹Sajjad Hussain and ²M. Anwar Kamal

¹Centre for Advanced Studies in Pure and Applied Mathematics, B. Z. Uni., Multan, Pakistan

²Department of Mathematics, King Suleiman Bin Abdul Aziz Uni., Saudi Arabia

Submitted: Aug 8, 2013; **Accepted:** Sep 14, 2013; **Published:** Oct 6, 2013

Abstract: The steady, incompressible micropolar fluid flow over a stretchable disk has been investigated. The governing partial differential equations have been transformed in to ordinary differential form by using similarity transformations. The resulting equations have been solved numerically, using SOR method and Simpson's (1/3) rule. The results have been improved by using Richardson's extrapolation. The velocity, micro rotation and pressure distributions have been obtained for various values of disk rotation parameter s for the range. Comparison of Newtonian and micropolar fluids flow is presented in tabular and graphical forms.

AMS Subject Classification: 76M20

Key words: Newtonian fluid • Micropolar fluid • Navier-stokes model • Stretchable disk • Extrapolation Method

INTRODUCTION

Eringen [1, 2] introduced the theory of micropolar fluids that provided enough generalization of the Navier-stokes model. Ariman *et al.* [3] discussed special features of micropolar fluids. Moreover, Lukaszewicz [4] and Eringen [5] provided extensive surveys of literature of the theory of micropolar fluids. Ishak *et al.* [6] examined the mixed convection of a micropolar fluid towards a stretching surface. Ali [7] studied the effect of variable viscosity on mixed convection heat transfer along a vertical moving surface. Mahapatra and Gupta [8] analyzed steady, two dimensional stagnation point flow of viscoelastic fluid towards a stretching surface. Kamal and Siaft [9] investigated the stretching of a surface in a rotating micropolar fluid. Kumar [10] presented a finite element solution of the problem of heat and mass transfer in a hyderomagnetic flow of a micropolar fluid past a stretching sheet. Guram and Anwar [11] considered the steady, laminar and incompressible flow of a micropolar fluid due to a rotating disk with suction and injection. Shafique and Rashid [12] obtained numerical solution of three dimensional micropolar fluid flows due to a stretching flat surface. Sajjad and Kamal [13] studied boundary layer flow for micropolar electrically

conducting fluid over a rotating disk in the presence of magnetic field. Chiam [14] investigated steady two dimensional stagnation point flow of an incompressible fluid towards a stretching surface.

Tiegang [15] presented an exact solution for Newtonian fluid flow over a stretchable disk for the range $0 \leq s \leq 500$. In this work, numerical solutions of this problem for micropolar fluids have been obtained for various values of disk rotation parameter s for the range $0 \leq s \leq 500$. If $s=0$, the flow corresponds to purely stretchable disk and when $s>0$, the flow is related to a stretching and rotating disk. The calculations have been carried out using three different grid sizes to check the accuracy of the results. The results of micropolar fluids are compared with the previous results where possible. The comparison is excellent. The numerical technique used in the present work is straightforward, economical and easy to program.

Mathematical Analysis: The problem under consideration is solved with the following assumptions; the flow is steady and incompressible, the cylindrical coordinates (r, θ, z) are used, r being the radial distance from the axis, θ the polar angle and z the normal distance from the disk, the body force and the body couple are neglected.

Under these assumptions the basic equations of motion given by Eringen [2] become:

$$\nabla \cdot \underline{V} = 0 \quad (1)$$

$$-(\mu + \kappa) \nabla \times (\nabla \times \underline{V}) + \kappa (\nabla \times \underline{V}) - p + \underline{J} \times \underline{B} = \rho (\underline{V} \times \nabla) \underline{V} \quad (2)$$

$$(a + \beta + \gamma) \nabla (\nabla \cdot \underline{V}) - \gamma (\nabla \times \nabla \times \underline{V}) + \kappa (\nabla \times \underline{V}) - 2\kappa \underline{v} = \rho j (\underline{V} \cdot \nabla) \underline{v} \quad (3)$$

$\underline{V} = V(u, v, w)$ is the velocity and the spin velocity vector is $\underline{v} = v(v_1, v_2, v_3)$. Also, p is the pressure, j the micro-inertia, α , β , γ and κ are material constants.

Now, using the following similarity transformations:

$$u = r\omega F(\eta), v = r\omega G(\eta), w = \sqrt{\omega v} H(\eta), p = \rho v \omega P(\eta)$$

$$v_1 = -(r\omega^{3/2}/v^{1/2})L(\eta), v_2 = (\frac{r\omega^{3/2}}{v^{1/2}})M(\eta), v_3 = 2\omega N(\eta), \quad (4)$$

where $\eta = \sqrt{\frac{\omega}{v}} z$ is the similarity variable, v being kinematics viscosity. The continuity equation is identically satisfied. The equations (2) to (3) in dimensionless form become:

$$2F + H' = 0, \quad (5)$$

$$F^2 - G^2 + HF' - (1 + C_1)F'' + C_1 M' = 0, \quad (6)$$

$$2FG + HG' - (1 + C_1)G'' + C_1 L' = 0, \quad (7)$$

$$-HH' - 2(1 + C_1)F'' + 2C_1 M = P'. \quad (8)$$

$$C_3 L'' + C_1 C_2 G' - 2C_1 C_2 L = FL + HL' + GM, \quad (9)$$

$$C_3 M'' + C_1 C_2 F' - 2C_1 C_2 M = 2FM + HM', \quad (10)$$

$$C_4 N'' + (C_3 - C_4)L' + C_1 C_2 G - 2C_1 C_2 + HN' = 0, \quad (11)$$

where primes denote differentiation with respect to η and C_1, C_2, C_3, C_4 are dimensionless constants, given as:

$$C_1 = \frac{\kappa}{\mu}, C_2 = \frac{\mu}{\rho j \omega}, C_3 = \frac{\gamma}{\rho j v}, C_4 = \frac{\alpha + \beta + \gamma}{\rho j v},$$

The boundary conditions are:

$$\eta = 0 : F = 0, G = s, H = 0, P = 0, L = 0, M = 0, N = 0, \quad (12)$$

$$\eta \rightarrow \infty : F = 0, G = 0, L = 0, M = 0, N = 0, \quad (12)$$

where, s is the disk rotation parameter which shows the disk rotation strength relative to the disk stretching strength. It is to be noticed that the similarity equations are obtained when the disk stretching speed is proportional to radius of the disk. The problem reduces to Newtonian fluid flow problem Teigang [15] for vanishing micro rotation v and κ .

Computational Procedure: The equations (6) to (7) and (9) to (11) are approximated by using central differences at a typical point $\eta = \eta_n$ of the interval $[0, \infty)$. For computational purposes, the interval $[0, \infty)$ is replaced by $[0, b]$, where b is a sufficiently large.

Then the finite difference equations are solved numerically by using SOR method Smith [16, p.262] at each required grid point of interval $[0, b]$ subject to the appropriate boundary conditions. The equation (5) is integrated by using Simpson's (1/3) rule Gerald [17, p.293] along with the formula given in Milne [18, p.48]. Higher order accuracy $O(h)^6$ on the basis of above solutions is achieved by Richardson's extrapolation Burden [19, p.168]. The pressure equation (8) is integrated by using initial condition $P(0) = 0$.

RESULTS AND DISCUSSIONS

The calculations have been carried out for different values of the parameter s namely $s=0.0$ and $0 < s \leq 500$ for three different grid sizes namely $h=0.025, 0.0125$ and 0.006 . Also, the results have been calculated for three different sets of material constants, chosen arbitrarily which are given below.

Cases	C_1	C_2	C_3	C_4
I	0.1	0.2	3.0	2.0
II	1.0	2.0	4.0	5.0
III	0.01	0.2	3.0	2.0

When the disk rotation parameter $s=0$, the problem corresponds to a flow over a stretchable disk only. In this situation, the stretching of the disk in the radial direction causes the flow, hence there is no flow in the circumferential direction and the value of G remains zero. The numerical solutions for the radial and axial

Table 1: comparison of the values of $H(\infty)$ for large s

S	Previous results Tiegang [15]	Present results (Newtonian fluids)	Micropolar fluids
100.0	8.84	8.8778	8.9143
150.0	10.82	10.8808	10.9226
200.0	12.50	12.5439	12.6065
250.0	-----	14.0166	14.0864
300.0	-----	15.3485	15.4251
350.0	-----	16.5733	16.6553
400.0	-----	17.7136	17.8011
450.0	-----	18.7852	18.8773
500.0	-----	19.7964	19.8953

Table 2: comparison of the values of $-P(\infty)$ for large s

S	Previous results Tiegang [15]	Present results (Newtonian Fluids)	Micropolar fluids
100.0	39.06	37.4083	37.7326
150.0	58.59	57.1959	57.6525
200.0	78.12	76.6749	77.4627
250.0	-----	96.2336	97.2144
300.0	-----	115.7891	116.9680
350.0	-----	135.34	136.6997
400.0	-----	154.8864	156.4395
450.0	-----	174.4422	176.1755
500.0	-----	193.93	195.9120

Table 3: $s = 0$, Numerical Results using SOR Method and Simpson's Rule for grid size $h=0.006$

η	F	H	P	L
0.000	1.000000	0.000000	0.000000	0.000000
0.300	0.699009	-0.505523	0.474205	0.134695
0.600	0.476719	-0.854604	0.681388	0.253212
0.900	0.319511	-1.090615	0.766258	0.343645
1.200	0.211637	-1.247872	0.798134	0.399368
1.500	0.138884	-1.351582	0.808845	0.417850
1.800	0.089957	-1.419277	0.812913	0.399303
2.100	0.056540	-1.462616	0.817298	0.345544
2.400	0.032808	-1.489049	0.825750	0.259171
2.700	0.014825	-1.503126	0.840656	0.143047
3.000	0.000000	-1.507464	0.863775	0.000000

Table 4: Numerical Results using SOR Method for finer grid size $h=0.006$, $s=5$

η	F	G	H	P	L	M	N
0.0	1.000000	5.000000	0.000000	0.000000	0.000000	0.000000	0.000000
0.5	1.017989	1.871126	-1.175958	-0.727417	-0.017094	0.112977	-0.016507
1.0	0.448643	0.641922	-1.890274	-0.683855	-0.019234	0.212741	0.287117
1.5	0.158445	0.206567	-2.172789	-0.677397	-0.012785	0.233145	0.396705
2.0	0.044574	0.053773	-2.265228	-0.654775	-0.005483	0.157709	0.259651
2.5	0.000000	0.000000	-2.284328	-0.609077	0.000000	0.000000	0.000000

Table 5: Numerical Results using SOR Method for finer grid size $h=0.006$, $s=100$

η	F	G	H	P	L	M	N
0.0	1.000000	100.000000	0.000000	0.000000	0.000000	0.000000	0.000000
0.5	1.297483	1.718421	-9.022668	-41.299223	-0.052691	0.713748	0.862461
1.0	0.027209	0.024428	-9.333478	-41.611325	-0.012990	0.844620	0.428229
1.5	0.006760	0.000307	-9.345458	-41.682302	-0.002654	0.622084	0.112721
2.0	0.003394	-0.000003	-9.350504	-41.722747	-0.000461	0.319838	0.021568
2.5	0.000000	0.000000	-9.352211	-41.731926	0.000000	0.000000	0.000000

Table 6: Numerical Results using SOR Method for finer grid size $h=0.006, s=300$

η	F	G	H	P	L	M	N
0.0	1.000000	300.000010	0.000000	0.000000	0.000000	0.000000	0.000000
0.2	13.608695	19.273731	-14.143405	-125.235330	-0.048767	0.378554	0.279708
0.4	0.793266	1.033039	-15.978007	-127.234870	-0.023089	0.603185	0.301228
0.6	0.045212	0.055114	-16.081613	-127.399570	-0.007546	0.506174	0.142478
0.8	0.003786	0.002786	-16.087976	-127.419060	-0.001918	0.276493	0.043261
1.0	0.000000	0.000000	-16.088555	-127.420810	0.000000	0.000000	0.000000

Table 7: Numerical Results using SOR Method for finer grid size $h=0.006, s=500$

η	F	G	H	P	L	M	N
0.0	1.000000	500.000000	0.000000	0.000000	0.000000	0.000000	0.000000
0.2	10.207426	13.759872	-19.661907	-211.710140	-0.067500	0.879969	0.981061
0.4	0.247558	0.315170	-20.738935	-213.546840	-0.021831	1.268159	0.699686
0.6	0.010080	0.007179	-20.766049	-213.634580	-0.005276	0.986029	0.231293
0.8	0.002568	0.000154	-20.768041	-213.660920	-0.001053	0.516857	0.052595
1.0	0.000000	0.000000	-20.768539	-213.666120	0.000000	0.000000	0.000000

Table 8: Numerical Results using Richardson Extrapolation Method, $s = 0.2$

η	$h=0.025$	$h=0.0125$	$h=0.006$	Extrapolated		$h=0.025$	$h=0.0125$	$h=0.006$	Extrapolated
	F	F	F	F	η	G	G	G	G
0.000	1.000000	1.000000	1.000000	1.000000	0.000	0.200000	0.200000	0.200000	0.200000
0.500	0.542973	0.542406	0.541259	0.540787	0.500	0.098131	0.098154	0.098200	0.167873
1.000	0.271243	0.271422	0.271742	0.271873	1.000	0.046463	0.046467	0.046479	0.140651
1.500	0.122077	0.123130	0.125188	0.126033	1.500	0.020302	0.020289	0.020265	0.117634
2.000	0.042667	0.043812	0.046071	0.046999	2.000	0.006920	0.006908	0.006885	0.098200
2.500	0.000000	0.000000	0.000000	0.000000	2.500	0.000000	0.000000	0.000000	0.000000

Table 9: $s = 5.0$ $s=25$

η	Numerical Results using Richardson Extrapolation Method							
	$h=0.025$	$h=0.0125$	$h=0.006$	Extrapolated	$h=0.025$	$h=0.0125$	$h=0.006$	Extrapolated
F	F	F	F	η	F	F	F	F
0.000	1.000000	1.000000	1.000000	1.000000	0.000	1.000000	1.000000	1.000000
0.500	1.018752	1.018515	1.017989	1.017773	0.500	2.194403	2.195777	2.195798
1.000	0.448093	0.448282	0.448643	0.448792	1.000	0.296662	0.297181	0.297981
1.500	0.156070	0.156887	0.158445	0.159085	1.500	0.036272	0.037099	0.038620
2.000	0.042097	0.042942	0.044574	0.045244	2.000	0.004915	0.005518	0.006641
2.500	0.000000	0.000000	0.000000	0.000000	2.500	0.000000	0.000000	0.000000

Table 10: $s = 50.0$ $s=100$

η	Numerical Results using Richardson Extrapolation Method							
	$h=0.025$	$h=0.0125$	$h=0.006$	Extrapolated	$h=0.025$	$h=0.0125$	$h=0.006$	Extrapolated
F	F	F	F	η	F	F	F	F
0.000	1.000000	1.000000	1.000000	1.000000	0.000	1.000000	1.000000	1.000000
0.500	2.074054	2.075818	2.076155	2.076258	0.500	1.295994	1.297013	1.297483
1.000	0.112431	0.113156	0.114262	0.114712	1.000	0.024865	0.025957	0.027209
1.500	0.008548	0.009396	0.010749	0.011301	1.500	0.004748	0.005672	0.006760
2.000	0.002061	0.002569	0.003392	0.003728	2.000	0.002327	0.002813	0.003394
2.500	0.000000	0.000000	0.000000	0.000000	2.500	0.000000	0.000000	0.000000

Table 11: $s = 200$ $s=300$

η	Numerical Results using Richardson Extrapolation Method							
	$h=0.025$	$h=0.0125$	$h=0.006$	Extrapolated	$h=0.025$	$h=0.0125$	$h=0.006$	Extrapolated
F	F	F	F	η	F	F	F	F
0.000	1.000000	1.000000	1.000000	1.000000	0.000	1.000000	1.000000	1.000000
0.200	14.474019	14.534610	14.550860	14.556375	0.200	13.540448	13.592831	13.608695
0.400	1.522158	1.521526	1.521320	1.521247	0.400	0.796163	0.793677	0.793266
0.600	0.141726	0.141427	0.141350	0.141324	0.600	0.044980	0.045044	0.045212
0.800	0.012719	0.012812	0.012882	0.012910	0.800	0.003366	0.003615	0.003853
1.000	0.000000	0.000000	0.000000	0.000000	1.000	0.000000	0.000000	0.000000

Table 12: $s=400$ $s=500$

η	Numerical Results using Richardson Extrapolation Method							
	$h=0.025$	$h=0.0125$	$h=0.006$	Extrapolated	$h=0.025$	$h=0.0125$	$h=0.006$	Extrapolated
F	F	F	F	η	F	F	F	
0.000	1.000000	1.000000	1.000000	1.000000	0.000	1.000000	1.000000	1.000000
0.200	11.885790	11.917221	11.929817	11.934436	0.200	10.189950	10.196878	10.205141
0.400	0.436131	0.433335	0.433020	0.432949	0.400	0.249961	0.247587	0.247505
0.600	0.017414	0.017834	0.018189	0.018329	0.600	0.008467	0.009170	0.009672
0.800	0.001828	0.002189	0.002426	0.002519	0.800	0.001570	0.002019	0.002311
1.000	0.000000	0.000000	0.000000	0.000000	1.000	0.000000	0.000000	0.000000

components of velocity F, H , the pressure function P and microrotation L are presented in Table 3 for case-I. Graphically, the results of these functions are demonstrated in Fig. 1 for case-II. The negative direction of the axial velocity component H shows that the fluid is drawn towards the wall under the effect of wall stretching. The pressure near the disk is smaller than the pressure in the outer region. In fact, the pressure in the outer region pushes the fluid towards the wall. The numerical result in this study, for $F'(0) = -1.736802$, agrees with the previous result Tiegang [15] given as $F'(0) = -1.7221$.

If the rotation parameter $s > 0$, the problem corresponds to the flow over a rotating and stretching disk. The numerical results for velocity components F, G, H , the pressure function P and the microrotation components L, M, N are presented in Tables 4 to 7. The results of all these functions have also been calculated in the higher order accuracy $O(h^6)$ using Richardson extrapolation and are shown in the tables 8 to 12. The results for micropolar fluid have been compared with the results of Newtonian fluid and the results by Tiegang [15] in the tables 1 to 2. The comparison of the results is excellent.

Fig. 2 shows the radial velocity distribution. The radial velocity component near the disk exceeds the stretching velocity for increasing values of the rotation parameter. For smaller values of s , the disk stretching causes mainly the fluid flow in radial direction. For larger values of s , the fluid velocity over the disk becomes larger than the disk stretching speed under the increasing effect of centrifugal force. The axial velocity H increases in the negative z -direction for larger values of the rotation parameter due to the effect of disk rotation as shown in Fig. 3.

Also, for increasing values of the rotation parameter, the pressure decreases with the increase in the magnitude of the axial velocity. Fig. 4 and Fig. 5 depict the stretching shear force $F'(0)$ and rotational shear force $G'(0)$, for larger values of the parameter s . They increase with increasing values of s . Fig. 6, Fig. 7 and Fig. 8 exhibit comparison of micropolar and Newtonian fluids. It is observed that $F'(0)$, $G'(0)$ and H for micropolar fluids are lesser in value than for Newtonian fluids.

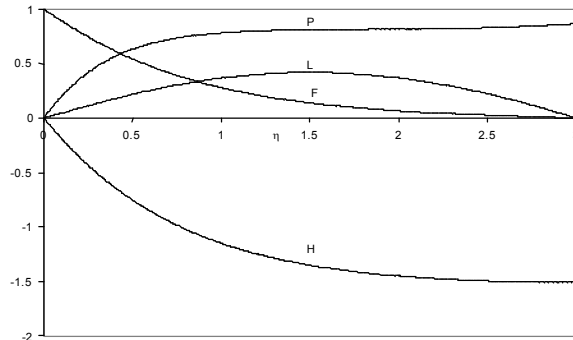


Fig. 1: Graph of F, H, P and L due to purely stretching disk when $s=0$

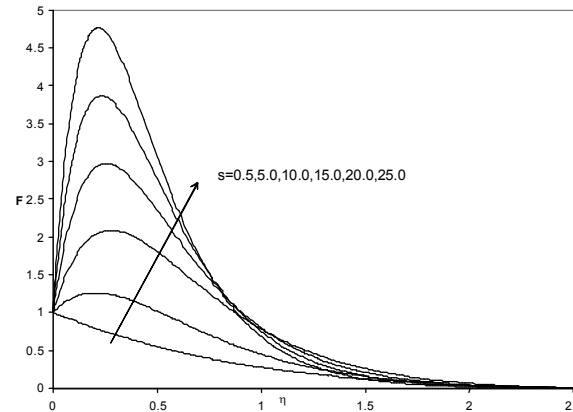


Fig. 2: Graph of F due to stretching and rotating disk for different values of s

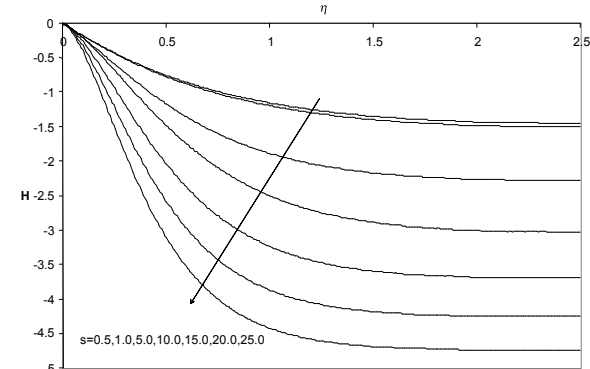


Fig. 3: Graph of H due to stretching and rotating disk for different values of s

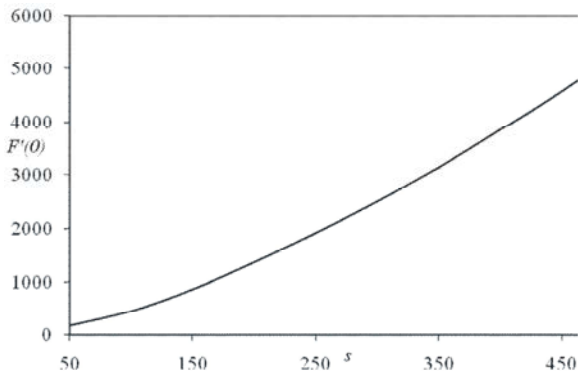


Fig. 4: Graph of $F'(0)$ for large values of s

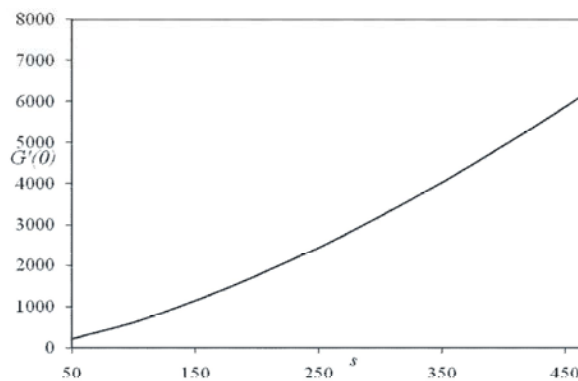


Fig. 5: Graph of $F'(0)$ for large values of s

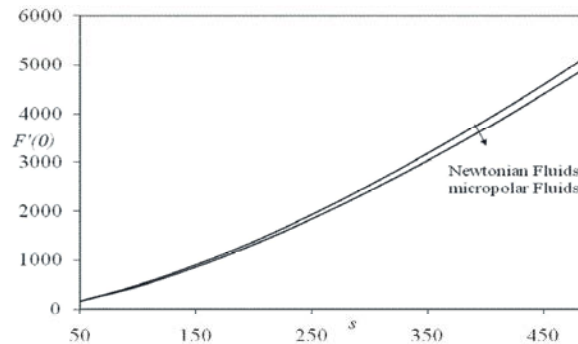


Fig. 6: Comparison of Newtonian and micropolar fluid flow

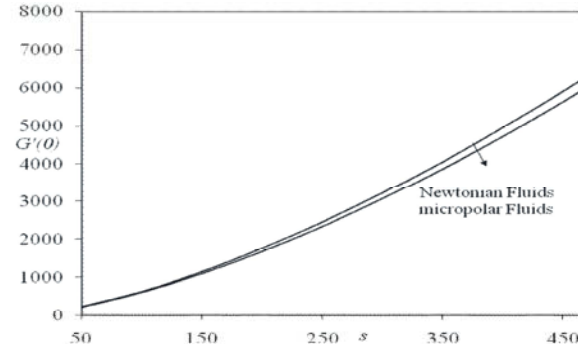


Fig. 7: Comparison of Newtonian and micropolar fluid flow

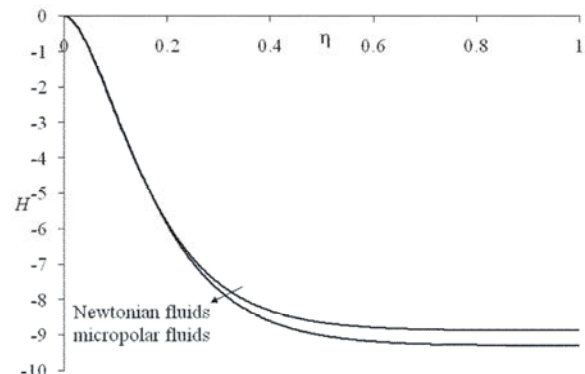


Fig. 8: Comparison of Newtonian and micropolar fluid flow.

CONCLUSION

Flow of micropolar fluid over a stretchable disk is discussed in detail. The constants "C's" affect the micro rotation of micropolar fluids flow. If one of these constants C_1 is close to zero the micropolar fluid flow resembles the Newtonian fluid flow.

It is observed that the stretching shear force $F'(0)$, rotational shear force $G'(0)$ and axial velocity component H for micropolar fluids are lesser in value than for Newtonian fluids.

REFERENCES

1. Eringen, A.C., 1964. Simple microfluid. Int. J. Eng. Sci., 2(2): 205-217.
2. Eringen, A.C., 1966. Theory of micropolar fluids. J. Math. Mech., 16(1): 1-18.
3. Ariman, T., M.A. Turk and N.D. Sylvester, 1973. Microcontinuum fluid mechanics- a review. Int. J. Eng. Sci., 11: 905-930.
4. Lukaszewicz, G., 1999. Micropolar Fluids: Theory and Application, Birkhauser, Basel.
5. Eringen, A.C., 2001. Microcontinuum Field Theories II: Fluent Media, Springer, New York.
6. Ishak, A., R. Nazar and I. Pop, 2008. Mixed convection stagnation point flow of a micropolar fluid towards a stretching surface. Mechanica, 43: 411-418.
7. Ali, M.E., 2006. The effect of variable viscosity on mixed convection heat transfer along a vertical moving surface. Int. J. Thermal Sci., 45: 60-69.
8. Mahapatra, T.R. and A.S. Gupta, 2004. Stagnation-point flow of viscoelastic fluid towards a stretching surface, Int. J. Non linear Mech., 39: 811-820.

9. Kamal, M.A. and S. Hussain, 1994. Steady flow of a micropolar in a channel with an accelerating surface velocity. *J. Natural Sciences and Mathematics*, 34(1): 23-40.
10. Lokendra, K., 2009. Finite element analysis of combined heat and mass transfer in hyderomagnetic micropolar flow along a stretching sheet. *Computational Material Science*, 46: 841-848.
11. Guram, G.S. and M. Anwar, 1981. Micropolar flow due to a rotating disk with suction and injection. *ZAMM*, 61: 589-595.
12. Shafique, M. and A. Rashid, 2006. Three dimensional micropolar flows due to a stretching flat surface. *Int. J. of Math. Analysis*, 1(2): 173-187.
13. Hussain, S. and M.A. Kamal, 2012. Magnetohydrodynamic boundary layer micropolar fluid flow over a rotating disk. *International Journal of Computational and Applied Mathematics*, 7(3): 301-13.
14. Chiam, T.C., 1994. Stagnation point flow towards a stretching plate. *J. Phys. Soc. Japan*, 63: 2443-2444.
15. Tiegang, F., 2007. Flow over a stretchable disk, *Physics of fluids*. 19: 1-4.
16. Gerald, C.F., 1989. *Applied Numerical Analysis*. Addison-Wesley Pub, New York.
17. Smith, G.D., 1979. *Numerical Solution of Partial Differential Equation*. Clarendon Press, Oxford.
18. Milne, W.E., 1970. *Numerical Solution of Differential Equation*, Dover Pub.
19. Burden, R.L., 1985. *Numerical Analysis*, Prindle, & Schmidt, Boston.